THE JOURNAL OF CHEMICAL PHYSICS **135**, 214503 (2011)

Manifestations of probe presence on probe dynamics in supercooled liquids

Stephan A. Mackowiak,[a] Jade M. Noble, and Laura J. Kaufman[b]
Department of Chemistry, Columbia University, New York, New York 10027, USA

(Received 24 August 2011; accepted 7 November 2011; published online 2 December 2011)

Experimental studies that follow behavior of single probes embedded in heterogeneous systems are increasingly common. The presence of probes may perturb the system, and such perturbations may or may not affect interpretation of host behavior from the probe observables typically measured. In this study, the manifestations of potential probe-induced changes to host dynamics in supercooled liquids are investigated via molecular dynamics simulations. It is found that probe dynamics do not necessarily mirror host dynamics as they exist either in the probe-free or probe-bearing systems. In particular, for a binary supercooled liquid, we find that smooth probes larger than the host particles induce increased translational diffusion in the host system; however, the diffusion is anisotropic and enhances caging of the probe, suppressing probe translational diffusion. This in turn may lead experiments that follow probe diffusion to suggest Stokes-Einstein behavior of the system even while both the probe-free and probe-bearing systems exhibit deviations from that behavior. © *2011 American Institute of Physics*. [doi:10.1063/1.3664125]

INTRODUCTION

The dynamics of supercooled liquids remain relatively poorly understood and have thus been the subject of continued study. One clear difference between typical and supercooled liquid dynamics is apparent in the non-exponential relaxations found in supercooled systems. Such relaxations are consistent with the presence of dynamic heterogeneity in these systems, and recent experiments and simulations on glass forming liquids in the supercooled regime support that these systems are dynamically heterogeneous.[1,2] While the presence of dynamic heterogeneity in small molecule supercooled liquids is thus largely agreed upon, detailing the size of these heterogeneous regions as well as the time scales over which they persist has been a topic of serious experimental focus in recent years, and results remain inconsistent at least in part because different experiments performed may probe different sub-ensembles of molecules and/or measure somewhat different quantities.[3–20]

Of experiments that investigate the length and time scales associated with heterogeneous dynamics in small molecule supercooled liquids, most utilize probes to follow dynamics in particular spatial or dynamical sub-ensembles of the supercooled liquid. While multi-dimensional NMR experiments use probes that differ from the host molecules only via isotopic labeling, most probe-bearing experiments are performed with fluorescent probes. In ensemble and some sub-ensemble experiments, fluorescent probes may be carefully chosen to resemble the host molecules in size and chemical functionality. To interrogate individual molecular scale environments, single molecule fluorescence approaches are utilized. These techniques require probe molecules of very high absorption cross section and fluorescence quantum yield. Such molecules tend to be large and conjugated and, as such, cannot generally be well matched in structure or size to the host molecules under study.

Using a probe that is large relative to the host molecules may affect probe ability to report the presence, size, and time scales associated with heterogeneous dynamics in the host – as those dynamics exist in the pure supercooled liquid – via several routes. First, as the probe becomes large compared to the size of the heterogeneous regions, the probe will span several regions, reporting only an average time scale. Additionally, as the probe becomes large, it also tends to become slow, and a slow probe may average over dynamic exchanges occurring in the system over time. The possibility that a large and/or slow probe may average over dynamic heterogeneities has been investigated in bulk and sub-ensemble experiments.[3,4,14,16,21–26] These experiments suggest that only probe molecules with similar hydrodynamic radius and mass to the supercooled liquid molecules can be expected to mirror dynamics and, in particular, dynamic heterogeneities in the surrounding system. One key finding was that for a set of probe/host molecules, all probes with mass $\geq$1.5 times that of the host molecule displayed single exponential relaxations even while solvation experiments on the supercooled liquid in the vicinity of the probes displayed non-exponential relaxations.[14] On the other hand, a recent single molecule study found heterogeneous dynamics reported in a probe/host system with mass ratio of probe to host of $>$8.[20] This discrepancy may reflect different extents of heterogeneous dynamics in the host supercooled liquids under study and/or differences in the experiments performed. Regardless of particular findings, it is clear that probes must average over dynamic heterogeneities when they are very large and/or slow compared to the size and/or persistence times of dynamic heterogeneities in the host system.

---

[a] Present address: Department of Chemistry, Ludwig-Maximilians-Universtat, Munich, Germany.

[b] Author to whom correspondence should be addressed. Electronic mail: kaufman@chem.columbia.edu.

Probe averaging over dynamic heterogeneities in supercooled liquids can thus occur and must be considered when interpreting results of probe-bearing studies; however, probe presence may also affect measurements in supercooled liquids in a more insidious fashion. The probe may perturb the local environment and local heterogeneous dynamics of the supercooled liquid and then preferentially report on that altered environment. Previous researchers have considered this possibility, and most single molecule fluorescence studies of supercooled liquids have refuted this idea through demonstration that the temperature dependence of probe rotation in the supercooled liquid mirrors that of the host as measured via viscosity or similar probe-free measurements.[17,18,20] While the rotational diffusion time of a probe tracking the viscosity of the host is a necessary condition if a probe is not altering the supercooled liquid dynamics, it is not sufficient to demonstrate that the probe is not altering the distribution of rotational or translational diffusion times of host molecules in the vicinity of the probe.

Though in experiments there are significant challenges to observing both host and probe behavior directly and simultaneously, this can be done with ease in simulation. Molecular dynamics simulations in a variety of probe-bearing supercooled and/or dense systems have been performed previously; however, there has been little explicit focus on the potentially reciprocal interactions between probe and host behavior.[27–40] Recently, we demonstrated that probes may alter host dynamics in supercooled liquids.[41] In this work, a binary Kob-Andersen (KA) supercooled liquid was simulated in the presence of smooth and rough probes with diameter 2 to 7 times that of the larger particles in the KA system. It was found that probes induced changes in the environment: smooth probes caused the mobility of particles in the first several solvation shells around the probe to increase, while rough probes induced the opposite behavior. While that work clearly demonstrated that probes may affect host dynamics, it did not follow the behavior of the probe in that altered environment, the only observable that can be tracked in most probe-bearing experiments. In this work, we follow probe behavior in environments affected by probe presence to further elucidate the information content of experiments using large probes in supercooled liquids.

SIMULATION DETAILS

A smooth spherical probe (p) is embedded in a supercooled liquid consisting of 3000 particles as described in an earlier study.[41] The model for the supercooled liquid is a binary mixture with a 4:1 ratio of A and B particles interacting via a Lennard-Jones (LJ) potential.[42–44] The LJ potential is given by $V_{\alpha\beta}(r) = 4\varepsilon_{\alpha\beta}[(\sigma_{\alpha\beta}/r)^{12} - (\sigma_{\alpha\beta}/r)^{6}]$, where $\alpha, \beta \in \{A, B, p\}$. The LJ parameters for the interaction between the A particles are $\sigma_{AA} = 1.0$ and $\varepsilon_{AA} = 1.0$ and between the B particles are $\sigma_{BB} = 0.88$ and $\varepsilon_{BB} = 0.5$. The LJ parameters for the interaction between the A and B particles are $\sigma_{AB} = 0.80$ and $\varepsilon_{AB} = 1.5$, ensuring that the system does not crystallize. The mass of the A and B particles is $m_A = m_B = 1.0$. The interaction of the probe with the A and B particles is determined by $\sigma_{px} = (\sigma_p + \sigma_x)/2$ with $\sigma_x = \sigma_{AA}$ or σ_{BB} and $\varepsilon_{px} = (\varepsilon_p + \varepsilon_x)^{1/2}$ with $\varepsilon_x = \varepsilon_{AA}$ or ε_{BB}. $\varepsilon_p = 1.0$ and $\sigma_p = 1.0$, 2.0, 3.0, 4.0, and 5.0. The mass of the probe is $m_p = 4.0$. The $\sigma_p = 1.0$ system is identical to a probe-free system except it contains a tagged particle of $\sigma_p = 1.0$ and $m_p = 4.0$, that is monitored in the same way probes in the other systems are monitored. The simulations are carried out, and the results are reported, in terms of the reduced variables $r^* = r/\sigma_{AA}$, $T^* = k_BT/\varepsilon_{AA}$, and $t^* = t(k_BT/m_A\sigma_{AA}{}^2)^{1/2}$. The interaction potentials and the corresponding forces in the range $3.0 \leq r^* \leq 4.0$ are interpolated from their LJ values at $r^* = 3.0$ to zero at $r^* = 4.0$ by a third-degree polynomial.

TABLE I. Parameters for systems investigated with $\sigma_p = 1 - 5$. P* is averaged over five simulations.

				P*			
σ_p	L*	ϕ^*	ρ^*	T* = 0.48	T* = 0.60	T* = 0.70	T* = 1.0
1.0	13.598	1.118	1.194	2.086	3.680	4.801	8.274
2.0	13.620	1.115	1.188	2.012	3.675	4.845	8.346
3.0	13.645	1.116	1.181	2.102	3.729	4.904	8.234
4.0	13.687	1.106	1.170	2.130	3.687	4.900	8.111
5.0	13.758	1.127	1.152	2.056	3.710	4.642	7.955

In our previous work, pressure ($P^* = P\sigma_{AA}{}^3/\varepsilon_{AA}$) was kept nearly constant as a function of temperature ($P^* \approx 2$ at $T^* = 0.48$ and $P^* \approx 3$ at $T^* = 0.70$) for all systems by changing the box volume ($V^* = L^{*3}$, with L* is the size of one side of the cubic box) with temperature (and probe size), resulting in somewhat different volume fractions ($\phi^* = (N_A {r^*_A}^3 + N_B {r^*_B}^3 + N_p {r^*_p}^3)/V^*$) and densities ($\rho^* = N/V^*$) for each system.[41] In this work, box size is also changed with probe size but not with temperature. In this formulation, volume fraction is kept constant across temperature, and pressure varies somewhat more with temperature but remains in a range such that pressure effects are not expected.[45] Specific values are given in Table I for the four temperatures investigated, T* = 1.0, 0.7, 0.6, and 0.48.

The molecular dynamics simulations are performed using GROMACS.[46,47] The system is equilibrated for at least 10^7 steps for each simulation using the Berendsen thermostat. The production runs are done in the microcanonical ensemble (N,V,E). For long time dynamics, simulations are performed with a time step of $dt^* = 0.01$ and 5×10^5 time steps for the highest temperature investigated and 1×10^7 time steps for the lowest temperature. A time step of $dt^* = 0.002$ is used for short time simulations. For each temperature and each probe size, five simulations from different initial configurations are performed to achieve good statistics.

RESULTS AND DISCUSSION

Structure and dynamics of the system

The structure of the probe-bearing systems is investigated via the radial distribution function (rdf), rdf = $g_{ij}(r) = dn_{ij}(r)/4\pi r^2 dr\rho_i$ with $i,j \in \{A,B\}$ and ρ density. The radial distribution functions $g_{AA}(r^*)$, $g_{AB}(r^*)$, and $g_{BB}(r^*)$ are virtually indistinguishable for the systems with probes of $\sigma_p = 1$–5, with the first and subsequent peaks in the same position in all cases and the height and width of the peaks

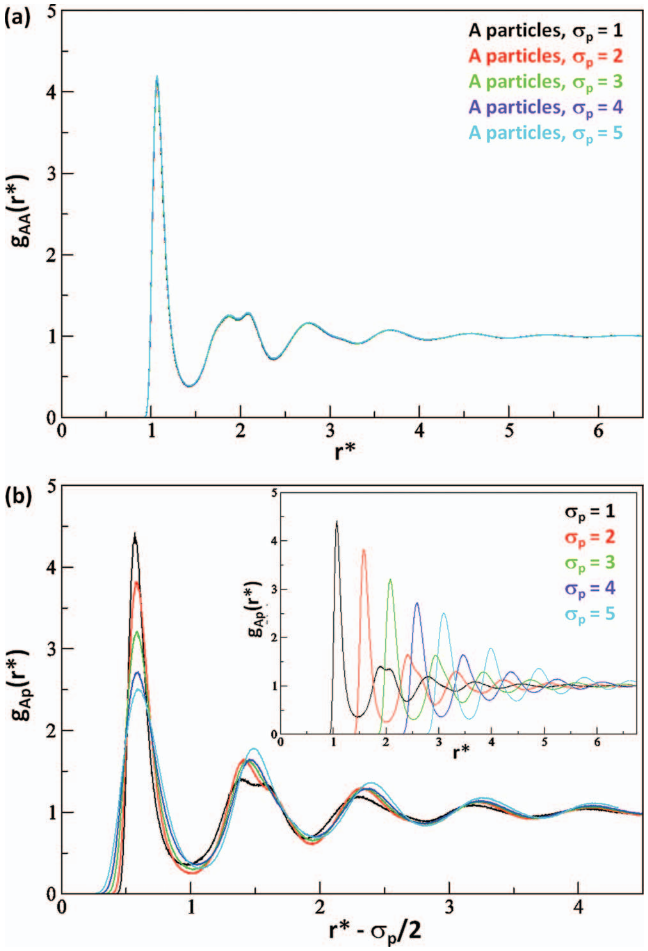

FIG. 1. (a) Radial distribution function (rdf) of A particles, $g_{AA}(r^*)$, in systems with probes of $\sigma_p = 1$ (black), $\sigma_p = 2$ (red), $\sigma_p = 3$ (green), $\sigma_p = 4$ (blue), $\sigma_p = 5$ (cyan) at $T^* = 0.48$. Rdfs are nearly identical and thus nearly completely overlap. (b) Rdfs of A particles relative to the probe $g_{Ap}(r^*)$ for $\sigma_p = 1$ (black), $\sigma_p = 2$ (red), $\sigma_p = 3$ (green), $\sigma_p = 4$ (blue), $\sigma_p = 5$ (cyan) at $T^* = 0.48$. Rdfs are shifted by σ_p /2 to highlight peak positions relative to the probe. The inset shows the unshifted $g_{Ap}(r^*)$ functions. Data is averaged over five simulations.

nearly identical (as shown in Fig. 1(a) for $g_{AA}(r^*)$), demonstrating that the bulk structure of these systems is insensitive to probe presence or size. More subtle differences in the structure of these systems can be ascertained by investigating the rdf of particles relative to the probes in the binary supercooled liquid, $g_{ip}(r) = \mathrm{d}n_{ip}(r)/4\pi r^2 dr\rho_i$ with $i \in \{\mathrm{A,B}\}$. The inset of Fig. 1(b) shows $g_{Ap}(r^*)$ for systems with $\sigma_p = 1$–5. Shifting each of the $g_{Ap}(r^*)$ functions by $\sigma_p/2$ reveals that the position of the first peak of the radial distribution functions is very similar relative to the probe, with a slight shift to the right with increasing probe size, from $r^*{-}\sigma_p/2 \approx 0.57$ for $\sigma_p = 1$ to ≈ 0.59 for $\sigma_p = 5$ (Fig. 1(b)). While this difference is subtle, the height and width of the first peaks are noticeably different, with the peak becoming lower and broader with increasing probe size. Additionally, subsequent peaks in the radial distribution function change, with a loss of the split in the second peak seen for all probes of $\sigma_p \geq 2$ and slight shifts to the right for all peak positions with increasing probe size. The decrease in height and increase in width of the first peak as well as the loss of split in the second peak seen in $g_{Ap}(r^*)$ with increasing probe size are indicative of a less glassy environment than is reflected in $g_{Ap}(r^*)$ for $\sigma_p = 1$ (or the identical $g_{AA}(r^*)$) at this temperature. This is consistent with the finding that the first peak of the radial distribution function becomes lower and broader with increasing temperature in the KA system.[42]

The fact that a $\sigma_p \geq 2$ probe-bearing system at $T^* = 0.48$ appears less glassy as assessed by $g_{Ap}(r^*)$ than a probe-free system at this temperature suggests that the particles in the probe-bearing system may be more mobile than are those in a probe-free KA system at this temperature. The dynamics of the probe-bearing binary liquids are first characterized by mean square displacement (MSD), which yields a diffusion constant D. The MSD is calculated according to MSD $= \langle r^2(t)\rangle = \langle (1/N)\sum (r_j(0) - r_j(t))^2\rangle$, where $r_j(t)$ is the position of particle j at time t, and the sum is over all particles, N. Figure 2(a) shows the MSDs of A particles in systems with probes of $\sigma_p = 1$–5 at $T^* = 0.48$. The MSDs are consistent with the system being in the supercooled regime at this temperature as is demonstrated by the presence of a plateau at intermediate times indicating caging behavior. At long times, the MSDs become linear, indicating diffusive behavior. Diffusion constants are obtained by fitting this long-time linear region to a line whose slope is $6D_{\mathrm{A(p)}}$, with $D_{\mathrm{A(p)}}$ the diffusion constant of the large A particles in a system bearing a $\sigma_p = \mathrm{p}$ probe. As described in the previous work, a smooth spherical probe larger than the A particles induces an increase in translational diffusion of the particles surrounding the probe.[41] The diffusion constants for these systems are shown in Fig. 2(c). The same trend is found for B particles (data not shown).

The dynamics of the probe-bearing binary liquids can also be characterized by the self part of the intermediate scattering function, $F_s(q,t)$, which yields the alpha-relaxation time, τ_α. The self part of the intermediate scattering function is given by $F_s(q,t) = \langle (1/N)\sum e^{iq[r_j(t)-r_j(0)]}\rangle$, where $r_j(t)$ is the position of particle j at time t.[48] The wavevector for the A particles at which $F_s(q,t^*)$ is calculated is $q = 7.25$, the peak of the static structure factor of these systems regardless of probe size. Figure 2(b) shows the self-intermediate scattering function for the A particles for systems in the presence of probes of various sizes at $T^* = 0.48$. From $F_s(q,t^*)$ we obtain the alpha-relaxation time, $\tau_{\alpha,\mathrm{A(p)}}$, defined as the time when the $F_s(q,t^*)$ of the A particles in a system with a probe of $\sigma_p = \mathrm{p}$ decays to its $1/e$ value. Consistent with the increase of diffusion constant of large A particles as a function increasing probe size, $\tau_{\alpha,\mathrm{A(p)}}$ decreases with increasing probe size. The alpha-relaxation times as a function of probe size are shown in Fig. 2(c). The same trend is found for B particles (data not shown).

As described in Ref. 41, the accelerated dynamics seen in the binary supercooled liquid in the presence of large, smooth probes disappears in the limit of an infinite system. The increase of diffusion constant and decrease of alpha-relaxation time for the particles in probe-bearing systems is dominated by an increase in motion of particles in the first solvation shells around the probe. This effect decays as a function of distance from the probe. This was shown through the investigation of radially binned Debye Waller factors in Ref. 41 and is also consistent with the changes in the first several peaks of the radial distribution function for the A particles relative to the probes as shown in Fig. 1(b).

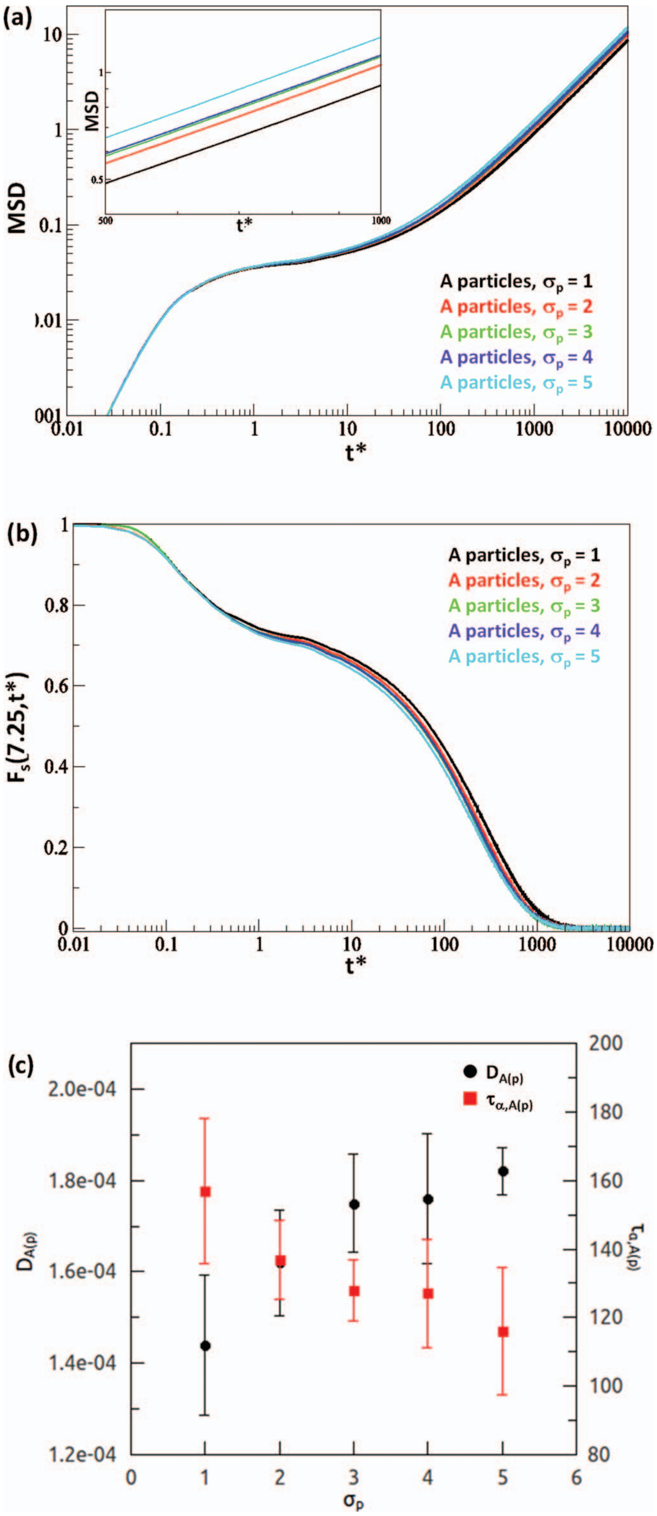

FIG. 2. (a) MSDs for A particles in systems with probes of $\sigma_p = 1$ (black), $\sigma_p = 2$ (red), $\sigma_p = 3$ (green), $\sigma_p = 4$ (blue), $\sigma_p = 5$ (cyan). Each MSD presented is the average of individual MSDs from five simulations. Inset shows a region of the MSDs in the linear, diffusive regime. (b) $F_s(q,t^*)$s for A particles in systems with probes from $\sigma_p = 1 - 5$ at $q = 7.25$, the peak of the static structure factor. Each $F_s(q,t^*)$ presented is the average of individual $F_s(q,t^*)$s from five simulations. Color scheme is the same as in (a). (c) Average translational diffusion constant, $D_{A(p)}$, (left axis, black circles) and average alpha-relaxation times, τ_α,$_{A(p)}$, (right axis, red squares) of large A particles in systems with $\sigma_p = 1 - 5$. Averages are obtained from the five simulations used to construct (a) and (b) and error bars are standard deviations over those five data sets.

Dynamics of the probe

Given the changes in the rdfs, MSDs, and $F_s(q,t^*)$s of probe-bearing supercooled systems that indicate that the systems become less glassy in the presence of probes of increasing size, it may be expected that the large probes themselves are more mobile at a given temperature than would be expected in a probe-free KA system at that temperature. To investigate this, we examine the MSDs and $F_s(q,t^*)$s of the probes themselves. Figure 3(a) shows the MSDs of large A particles in a $\sigma_p = 1$ system and of probe particles in systems with probes of $\sigma_p = 1 - 5$ at $T^* = 0.48$. The $\sigma_p = 1$ system is identical to a probe-free system except it contains a tagged particle of $\sigma_p = 1$ that is monitored in the same way probes in the other systems are monitored. As such, the MSDs for the A particles and the $\sigma_p = 1$ particle look very similar,

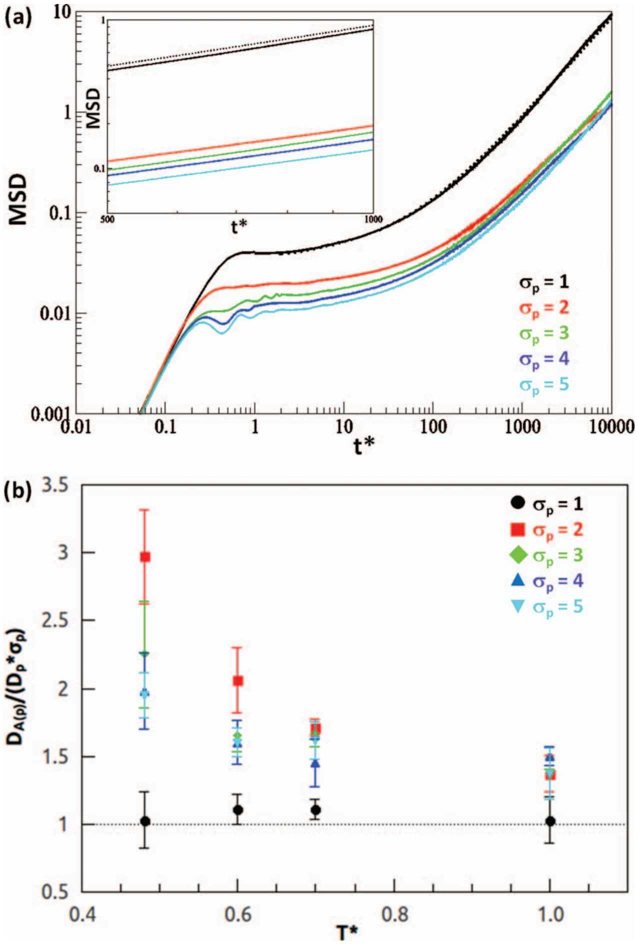

FIG. 3. (a) MSDs for probe particles in the same systems shown in Figs. 1 and 2, with $\sigma_p = 1$ (black), $\sigma_p = 2$ (red), $\sigma_p = 3$ (green), $\sigma_p = 4$ (blue), $\sigma_p = 5$ (cyan). Additionally, the MSD for the A particles (black dotted line) is shown. Each MSD presented is the average of individual MSDs from five simulations. Inset shows a region of the MSDs in the linear, diffusive regime. (b) Ratio of diffusion constant of the A particles for the system with probe of given size, σ_p, to the diffusion constant of the probe multiplied by the probe size as a function of temperature ($D_{A(p)}/(D_p{*}\sigma_p)$) for $\sigma_p = 1$ (black circles), $\sigma_p = 2$ (red squares), $\sigma_p = 3$ (green diamonds), $\sigma_p = 4$ (blue triangles), $\sigma_p = 5$ (cyan downward triangles). Positive deviations from 1 reflect probe motion that is decreased relative to motion of the A particles. Points are averages over five simulations and error bars are standard deviations.

with the $\sigma_{\rm p} = 1$ MSD demonstrating more noise, owing to the poorer statistics. For the larger probes ($\sigma_{\rm p} \geq 3$), oscillations are apparent in the short time regime of the probe MSDs, which is due to backscattering. For all MSDs, a plateau is evident at intermediate times, indicating that the probe behavior reflects the supercooled nature of the system. The height of the plateau of the MSD decreases with increasing probe size, indicating that the larger probes move within the cage less than the smaller probes. This is due to the large numbers of A and B particles surrounding the probes and imposing Brownian pressure. This trend is consistent with the trend between A and B particles for probe-free systems, where the larger particles move less in the cage and exhibit a lower plateau height than do the smaller particles. The values of the plateau height for the probes and the alterations in system dynamics as a function of probe size are reflected in $g_{\rm Ap}(r^*)$ (Fig. 1(b), inset), with the MSD plateau height inverse linearly related to the position of the first peak of $g_{\rm Ap}(r^*)$ for systems with $\sigma_{\rm p} = 2$–5.

To investigate whether the increased diffusion constants evident in the host particles of supercooled systems bearing large, smooth probes are also evident in the probes themselves, the long time, linear regime of the MSD (Fig. 3(a), inset) is investigated, and values for probe diffusion are extracted. First, given that the probes are of different size, even in identical environments a larger probe would be expected to be slower, with dimensionality arguments suggesting that $D_{\rm p} \sim \sigma_{\rm p}^{-1}$. As expected, the diffusion constants for the probes extracted from the MSDs do decrease with increasing probe size. Given that large smooth probes speed up the particles in the shells surrounding these probes, we investigate whether the slow down as a function of probe size is less than expected due to probe size alone via the quantity $D_{\rm A(p)}/(D_{\rm p}{}^*\sigma_{\rm p})$ (Fig. 3(b)). At $\sigma_{\rm p} = 1$, this quantity is near one regardless of temperature, as is expected, with deviations from 1 reflecting statistical error associated with tracking a single probe. At larger probe size, however, this quantity increases with decreasing temperature, indicating that the probe translational diffusion constant is smaller than would be expected based on probe size alone. Thus, even though the particles surrounding the probe exhibit increased diffusion constants due to the presence of the probe, the probe particles themselves do not experience a corresponding increase in diffusion and instead slow down relative to the particles in the surroundings. Because $D_{\rm A(p)}$ is dependent on system size, we also investigate $D_{{\rm A}(p=1)}/(D_{\rm p}{}^*\sigma_{\rm p})$ and find that the probe is unexpectedly slow even relative to the diffusion of large A particles in the $\sigma_{\rm p} = 1$ system. We note that although the $\sigma_{\rm p} = 1$ probe has $m_{\rm p} = 4$, the diffusion constant of this probe is identical to that of a $\sigma_{\rm p} = 1$, $m_{\rm p} = 1$ particle (data not shown). As such, this shows that the probe is unexpectedly slow even relative to the diffusion of large A particles in a probe-free system (or an infinitely large probe-bearing system, where $D_{\rm A(p)}$ would be equal to $D_{\rm A(p=1)}$).

Temperature dependence of probe dynamics

To further investigate probe dynamics, we evaluate the temperature dependence of probe behavior via both $D(T^*)$ and $\tau_\alpha(T^*)$. D is obtained from MSDs as described above. τ_α is obtained from $F_s(q,t^*)$. The wavevector at which the self-intermediate scattering function is evaluated for the probe particles is determined from the static structure factor between the probe and A particles of the probe-bearing systems. $F_s(q,t^*)$ of the probes is subsequently calculated at the peak wavevector ($q = 7.25$ for $\sigma_{\rm p} = 1$, $q = 5.40$ for $\sigma_{\rm p} = 2$, $q = 3.65$ for $\sigma_{\rm p} = 3$, $q = 2.80$ for $\sigma_{\rm p} = 4$, and $q = 2.25$ for $\sigma_{\rm p} = 5$).

To compare the temperature dependence of D for probes of various sizes, the diffusion constants were fit to the expression $D \propto (T - T_c)^\gamma$. Mode coupling theory predicts that the diffusion constant should follow such power-law behavior near a critical temperature, T_c.[49] Kob and Andersen previously found the best-fit to this expression using $T_c = 0.435$ and $\gamma = 2.0$ for the large A particles and $\gamma = 1.7$ for the small B particles.[42,50] In our slightly less dense $\sigma_{\rm p} = 1$ system, we find a very similar critical temperature and somewhat different values of γ. To find the best-fit T_c value, the probe diffusion temperature dependence for probes of each size $\sigma_{\rm p} = 1$–5 was fit to $D \propto (T - T_c)^\gamma$ allowing both T_c and γ to vary with probe size. The T_c values are then averaged, yielding $T_c = 0.436$. With this T_c value, all A particle, B particle, and probe diffusion data is well fit by the power-law expression (Fig. 4(a)). The A and B particles yield γ values of 1.71 and 1.51, respectively, somewhat lower than the values found by Kob and Andersen. This may be due to the lower density of the system studied here, the slightly different temperature range explored, and/or the fact that the power-law fits are relatively insensitive to small changes in γ.[51–53]

The values of γ obtained for the probe diffusion temperature dependence are given in Fig. 4(c). The value is maximal at $\sigma_{\rm p} = 2$ ($\gamma = 2.0$) and decreases with increasing probe size to $\gamma \approx 1.8$. Thus, the γ values for the temperature dependence of probe diffusion constants for probes of $\sigma_{\rm p} \geq 2$ are all greater than the 1.7 value obtained for large A particles in a $\sigma_{\rm p} = 1$ system and also higher than the values for large A particles in all probe-bearing systems ($\gamma = 1.6$–1.7, data not shown). Because the value of γ reports the degree of temperature dependence of diffusion, it is not unexpected that the γ values obtained from probe diffusion constants are greater than those obtained from diffusion constants of the A particles; indeed, this is consistent with the fact that the diffusion constant of the probe deviates from that of the large A particles, becoming slower faster than does the surrounding system with decreasing temperature, as shown in Fig. 3(b). Similarly, the fact that γ is maximal for $\sigma_{\rm p} = 2$ is consistent with the fact that the unexpected slow down in probe diffusion is maximal at $\sigma_{\rm p} = 2$ (Fig. 3(b)). We further validate the finding for $\sigma_{\rm p} = 2$ in a variety of manners. First, simulations for a $\sigma_{\rm p} = 1.5$ system are performed and diffusion constants for the probes are obtained and fit to the power-law functional form with $T_c = 0.436$. This yields a value of $\gamma = 1.87$, lower than only the $\sigma_{\rm p} = 2$ γ value. This suggests the high value obtained for γ for $\sigma_{\rm p} = 2$ is likely to represent a true increase relative to those found for larger probes. Additionally, probe diffusion data is also fit to a Vogel-Fulcher-Tamman expression $D \propto T\exp\left[-1/(K(T/T_o - 1))\right]$. Here $1/K$ is a measure of the temperature dependence of the diffusion, playing a

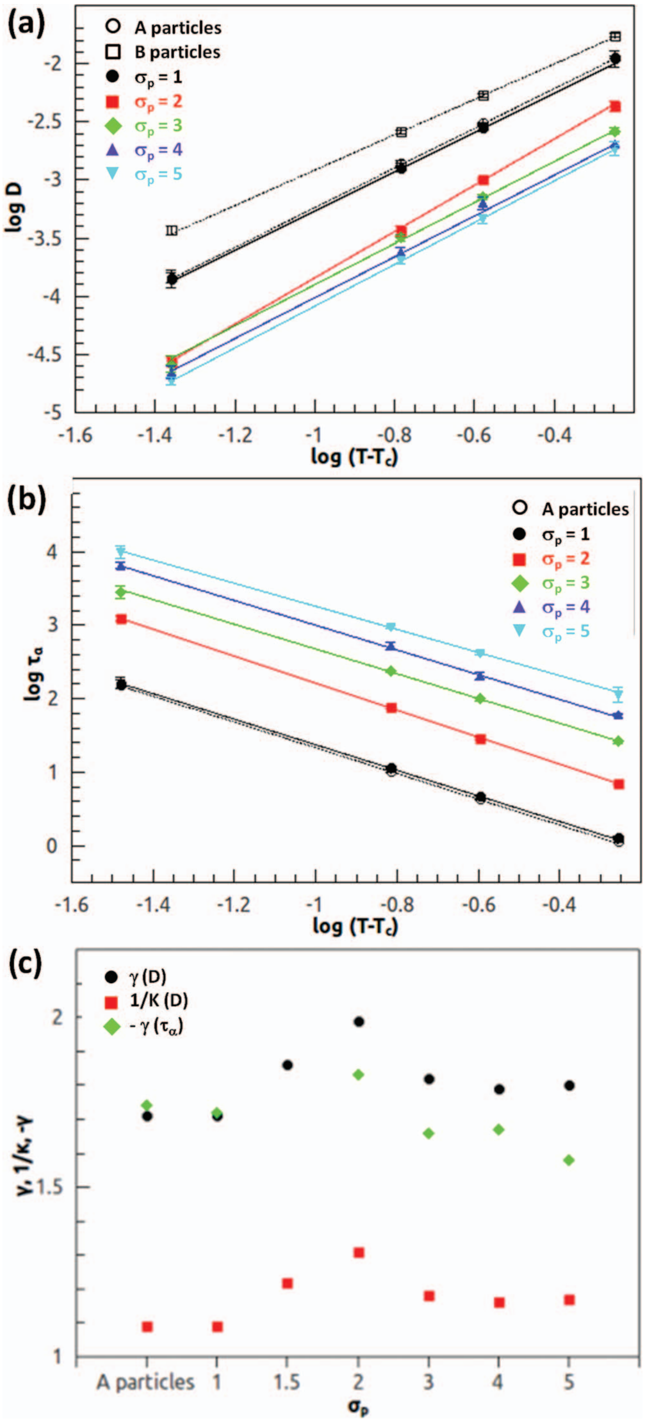

FIG. 4. (a) Temperature dependence of diffusion as expressed via log(D) vs log(T–T_c) for A particles in a $\sigma_{\mathrm{p}} = 1$ system (open black circles, dotted lines), B particles in a $\sigma_{\mathrm{p}} = 1$ system (open black squares, dashed line), and probe particles ($\sigma_{\mathrm{p}} = 1$, filled black circles; $\sigma_{\mathrm{p}} = 2$, red squares; $\sigma_{\mathrm{p}} = 3$, green diamonds; $\sigma_{\mathrm{p}} = 4$ blue triangles; $\sigma_{\mathrm{p}} = 5$, cyan downward triangles). Each point represents the average of diffusion constants over five simulations and error bars are standard deviations. $T_c = 0.436$ is the best-fit T_c value and was determined by finding the best-fit T_c for each of the data sets represented in the figure and then averaging those values. (b) Temperature dependence of alpha-relaxation as expressed via log(τ_α) vs. log($T - T_c$) for systems described in (a). Here $T_c = 0.447$, obtained via the same process described in (a). (c) Values of γ, $1/K$, and -γ as determined from fits to $D \sim (T - T_c)^{\gamma}$ (black circles; data and fits shown in (a)), $D \sim T\exp(-1/K(T/T_o-1)$ (red squares; data shown in (a); fits not shown), and $\tau_\alpha \sim (T - T_c)^{-\gamma}$ (green diamonds; data and fits shown in (b)), respectively. For fits to the Vogel-Fulcher-Tamman expression (red squares), $1/K$ values are best-fits for $T_o = 0.314$, determined in the same manner T_c values are determined.

role analogous to γ in the power-law expression.[53,54] T_o was set in the same manner as T_c, yielding a best-fit value of $T_o = 0.314$, similar to the value of $T_o = 0.324$ found previously for probe-free KA systems.[54] As shown in Fig. 4(c), the values of $1/K$ track the values of γ, with the maximum 1/K value again found at $\sigma_{\mathrm{p}} = 2$. Finally, we track the temperature dependence of the alpha-relaxation times of the probe by fitting probe data to the expression $\tau_\alpha \propto (T - T_c)^{-\gamma}$. As predicted by MCT, both the T_c and γ values should be the same for the power-law dependences of D and τ_α, though it was found in the probe-free KA system that for $T_c = 0.435$, the γ values were 2.5 and 2.6 for A and B particles, respectively, for τ_α (compared to 2.0 and 1.7, respectively, for D).[50] To achieve best-fits to the power-law, we allowed T_c to vary as described above, yielding $T_c = 0.447$, somewhat different from that found for D and, therefore, not in full agreement with the predictions of MCT. However, the γ value found for the power-law dependence of the A particles is nearly identical to that found for the fit of the diffusion constants. For the probe particles, the γ values do deviate somewhat from the γ values obtained for D, but the values track each other and again peak at $\sigma_{\mathrm{p}} = 2$. These results all support the finding that the probe dynamics in these systems do not change monotonically with probe size even while the particle dynamics do.

Probe dynamics relative to system dynamics

The origin of the surprising behavior indicating probes are slowing down more than would be expected based on size alone in the background of an increasingly mobile KA system can be understood by examining trajectories of particles surrounding the probe. Figure 5 displays two-dimensional projections of the trajectories of the A particles at $T^* = 0.48$ and $t^* = 500$ for single simulations with $\sigma_{\mathrm{p}} = 1$, 2, and 5. While the trajectories of the particles in the $\sigma_{\mathrm{p}} = 1$ system appear isotropic, those of particles surrounding the probes in the $\sigma_{\mathrm{p}} = 2$ and $\sigma_{\mathrm{p}} = 5$ systems appear anisotropic, with more motion along the probe than perpendicular to it. This was demonstrated qualitatively in the β- or caged regime in Ref. 41 and is shown for time scales associated with α-relaxation in Fig. 5. To examine this behavior quantitatively, the MSDs of the A particles in these systems are analyzed as a function of distance from the center of the probe (as defined at $t^* = 0$), in the frame rotated relative to the probe, yielding MSDs both parallel and perpendicular to the probe, as depicted in Fig. 6(a). The motion of the particles to and away from the probe is captured via the perpendicular mean square displacement, $\mathrm{MSD}_{\mathrm{perp}}$. The parallel mean square displacement, $\mathrm{MSD}_{\mathrm{par}}$, represents the remaining motion, which captures motion along the probe both in and out of the plane. Figure 6(a) shows the total MSD values as well as the parallel and perpendicular MSD values at $t^* = 50$ (multiplied by 5) and $t^* = 500$ at $T^* = 0.48$ for systems with $\sigma_{\mathrm{p}} = 1$ as a function of distance from the probe. For $\sigma_{\mathrm{p}} = 1$ probes, these values do not change substantially as a function of distance from the probe, as expected. Moreover, the value of the parallel MSD is approximately two times the value of the perpendicular MSD, as is expected for isotropic motion since

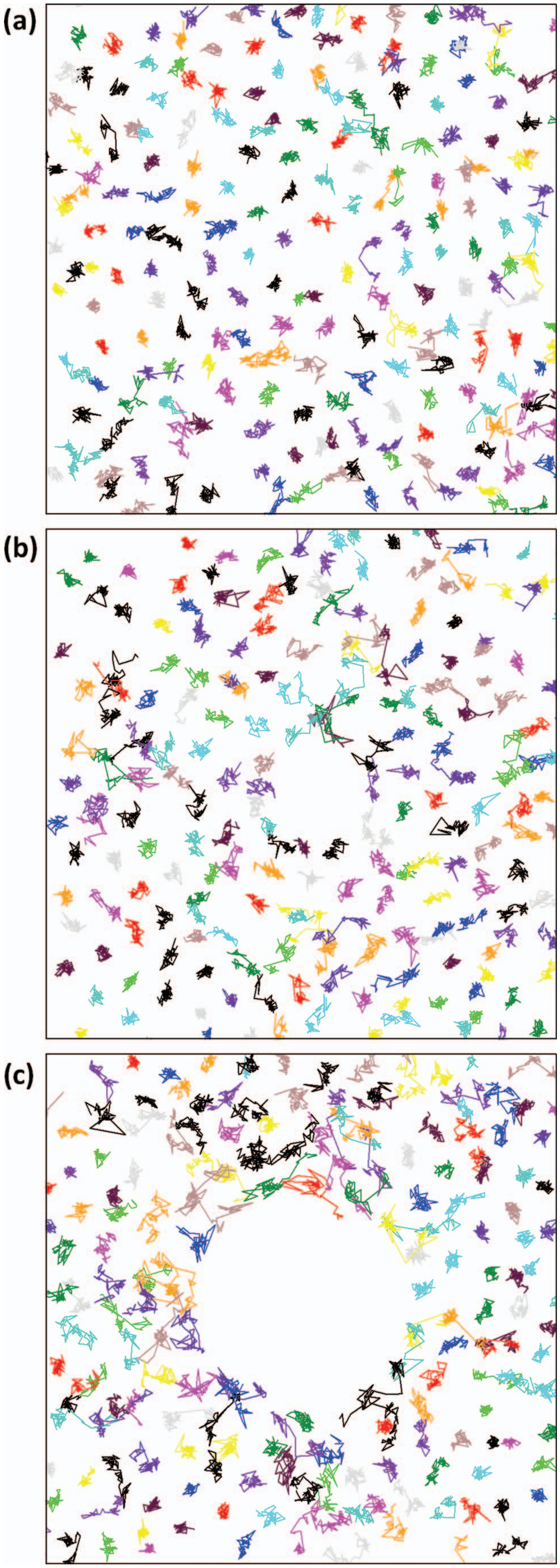

FIG. 5. 2D projections of 3D trajectories of large A particles at $T^* = 0.48$ surrounding a (a) $\sigma_p = 1$ probe (b) $\sigma_p = 2$ probe, and (c) $\sigma_p = 5$ probe all at $t^* = 500$ with frames separated by $dt^* = 20$.

$\text{MSD} = (\text{MSD}_x + \text{MSD}_z) + \text{MSD}_y = \text{MSD}_{par} + \text{MSD}_{perp}$. Figures 6(b) and 6(c) show these same quantities for systems with $\sigma_p = 2$ and $\sigma_p = 5$, respectively. For $\sigma_p = 2$, the total and parallel MSD values are greater than in the $\sigma_p = 1$ system, especially at $t^* = 500$, while the perpendicular values are not. This is consistent both with the increase in diffusion constant in large A particles shown in Fig. 2(c) and the presence of anisotropic mobility in the system with enhanced motion along the probe. At $\sigma_p = 5$, these trends are more evident at both $t^* = 50$ and $t^* = 500$. Additionally, it becomes clear that the particle motion is not enhanced uniformly throughout the system. At $t^* = 500$, while there is still an enhancement in total MSD of a factor of ≈ 1.4 at the furthest distance from the probe, the enhancement is greater than a factor of 3 adjacent to the probe. The enhancement is also most anisotropic near the probe, with the parallel motility enhanced by a factor of nearly 4 over that in the $\sigma_p = 1$ system while the perpendicular enhancement is less than a factor of 2. At both $\sigma_p = 2$ and $\sigma_p = 5$, there is some evidence of not only enhanced motility along the probe for particles adjacent to the probe but also slightly decreased motility perpendicular to the probe relative to that seen at larger distances from the probe. This is likely due to the fact that as the probe itself grows larger, it grows slower and particles nearest the probe have restricted motion towards the probe. However, even given that effect, the more obvious effect is an increase of MSD_{par}, which is both more substantial than the decrease in MSD_{perp} and persists to further distances from the probe. To demonstrate how the anisotropy in diffusion manifests as a function of probe size, the ratio $\text{MSD}_{par}/\text{MSD}_{perp}$ is plotted as a function of distance from the probe for systems with $\sigma_p = 1$–5 in Fig. 6(d). As is consistent with Fig. 6(a), for systems with $\sigma_p = 1$, $\text{MSD}_{par}/\text{MSD}_{perp}$ is ~ 2 at all distances from the probe at both $t^* = 50$ and $t^* = 500$. However, with increasing probe size, the ratio increases near the probe. This behavior is similar to that which has been seen in some simulations of supercooled systems near smooth walls, in which the particles near the wall speed up and do so in an anisotropic manner.[55–58]

To further investigate how the behavior of the particles around the probe may influence the behavior of the probe itself, we investigate how the maximum value of $\text{MSD}_{par}/\text{MSD}_{perp}$ varies with probe size. Indeed, while the anisotropy of the motility of the particles surrounding probes explains how the diffusion constant of the probe may decrease (more than expected from size alone) even while that of the particles in the surroundings increase, it does not explain why this behavior is most obvious in the $\sigma_p = 2$ system and in fact becomes less prominent as a function of increasing probe size (Figs. 3(b) and 4). One possibility is that the degree of anisotropy does not increase substantially with increasing probe size, but this does not appear to be the case: indeed the maxima of $\text{MSD}_{par}/\text{MSD}_{perp}$ at both $t^* = 50$ and $t^* = 500$ increases nearly linearly with probe size (Fig. 6(e)). Another possibility is that a set of competing factors is at play. For the largest probes studied, even though there is a tendency for the probes to be more fully caged because of particles moving around the probe tangentially, this may be counterbalanced by the fact that at large probe size the surroundings

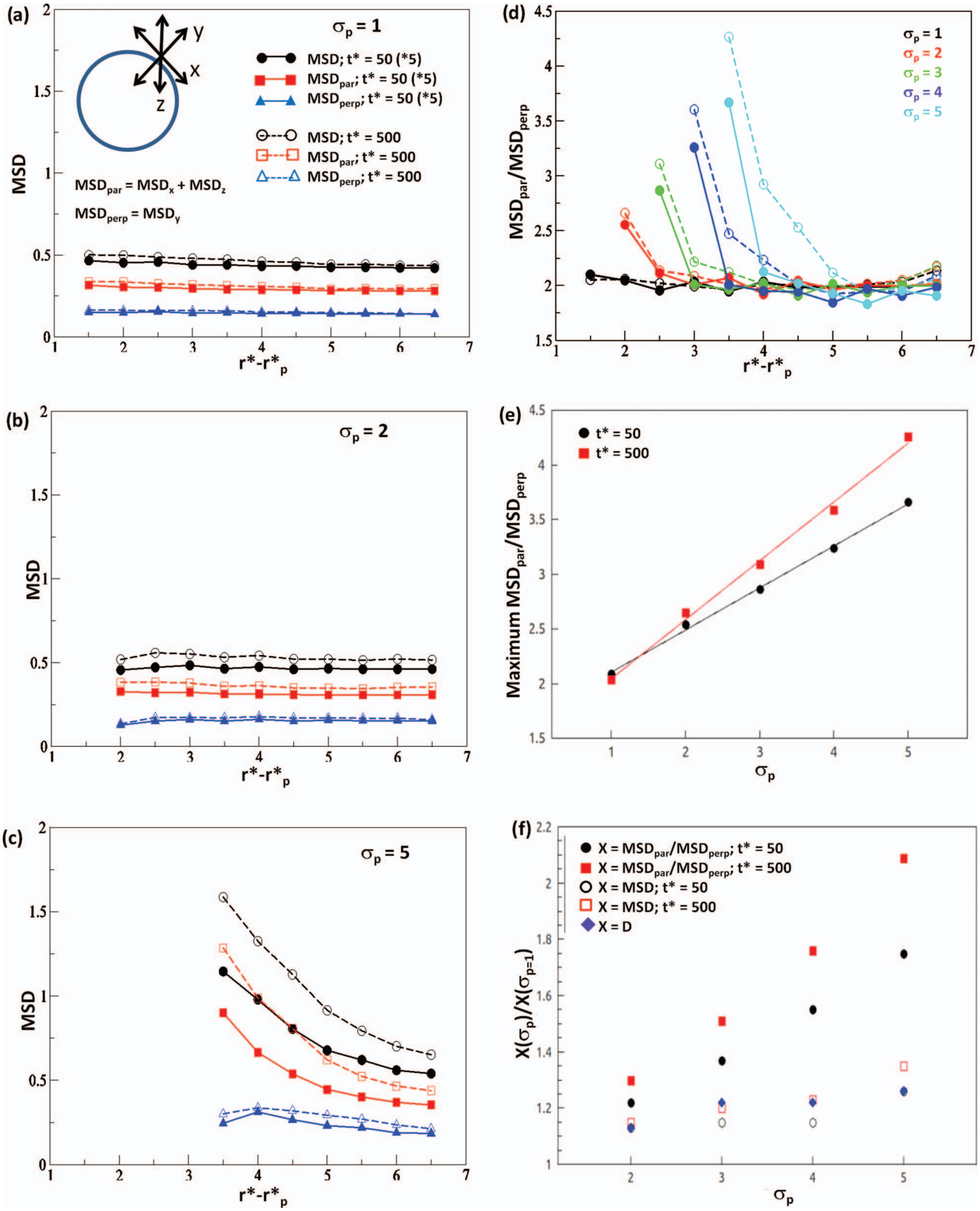

FIG. 6. MSD values as a function of distance from the probe to particle centers (defined at $t^* = 0$), for (a) $\sigma_p = 1$, (b) $\sigma_p = 2$, and (c) $\sigma_p = 5$. Figure 6(a) also shows the rotated frame relative to the probe, with $\mathrm{MSD}_{par} = \mathrm{MSD}_x + \mathrm{MSD}_z$ and $\mathrm{MSD}_{perp} = \mathrm{MSD}_y$. In (a)–(c), solid lines with filled symbols are values at $t^* = 50$, all multiplied by 5, and dashed lines with open symbols are values at $t^* = 500$. Black lines and black circles represent total MSD values, red squares and red lines represent MSD_{par} values, and blue lines and symbols represent MSD_{perp} values. (d) Ratio of MSD values parallel and perpendicular to the probe ($\mathrm{MSD}_{par}/\mathrm{MSD}_{perp}$) at $t^* = 50$ (solid lines and filled symbols) and $t^* = 500$ (dashed lines and open symbols) as a function of distance from the probe for probes of $\sigma_p = 1$ (black), $\sigma_p = 2$ (red), $\sigma_p = 3$ (green), $\sigma_p = 4$ (blue), and $\sigma_p = 5$ (cyan). (e) Maximum values of binned $\mathrm{MSD}_{par}/\mathrm{MSD}_{perp}$ values from (d) as a function of probe size for $t^* = 50$ (black circles) and $t^* = 500$ (red squares). Best-fit lines are shown. (f) Various quantities (X) normalized by those quantities for the $\sigma_p = 1$ system: X = Maximum values of binned $\mathrm{MSD}_{par}/\mathrm{MSD}_{perp}$ values at t* = 50 (filled black circles) and t* = 500 (filled red squares), total MSD values for those systems at $t^* = 50$ (open black circles) and $t^* = 500$ (open red squares), and the diffusion constants obtained from the full MSDs (filled blue diamonds). All data in Fig. 6 are attained from an average of two simulations performed at each probe size.

speed up most appreciably, with that acceleration extending to further distances from the probe. Thus at large probe size, the caging problem is mitigated by the overall increased mobility of the surrounding particles whereas at smaller probe size the increased caging is not as strongly counterbalanced by the increased particle mobility. To investigate whether this is the case, the maxima of $\mathrm{MSD}_{\mathrm{par}}/\mathrm{MSD}_{\mathrm{perp}}$ for systems with probes of $\sigma_{\mathrm{p}} = 2$–5 relative to the maximum of this quantity for the $\sigma_{\mathrm{p}} = 1$ system is plotted (Fig. 6(f)). As expected, this quantity also increases approximately linearly at both $t^* = 50$ and 500. To compare this to the potentially counterbalancing effect of the increased overall mobility of the surroundings, we plot $D_{\mathrm{A(p)}}/D_{\mathrm{A(p=1)}}$. Because the diffusion constant increase need not track the actual values of the MSD at $t^* = 50$ and 500, we also plot the values of the MSD for the large A particles (Fig. 2(a)) for systems with $\sigma_{\mathrm{p}} = 2$–5 relative to that with $\sigma_{\mathrm{p}} = 1$ at these times. We find that the values of the MSD at $t^* = 50$ and 500 do track the diffusion constant. Moreover, despite the fact that the overall D and MSD values do increase with probe size, the maximal anisotropy increases more quickly with probe size; thus, we do not find clear evidence that the competing factors identified lead to the slowdown of the probe being most appreciable in the $\sigma_{\mathrm{p}} = 2$ probe-bearing system. However, it is apparent in Fig. 6(e) that there is some deviation from linear behavior in the maxima of $\mathrm{MSD}_{\mathrm{par}}/\mathrm{MSD}_{\mathrm{perp}}$ as a function of probe size, with a positive deviation apparent at $\sigma_{\mathrm{p}} = 2$. Additionally, Figs. 6(a) and 6(b) reveal that near the $\sigma_{\mathrm{p}} = 2$ probe, $\mathrm{MSD}_{\mathrm{par}}$ increases while $\mathrm{MSD}_{\mathrm{perp}}$ actually decreases relative to that for the $\sigma_{\mathrm{p}} = 1$ system, and this is the only probe size for which this occurs. As such, the degree of enhanced caging of the probe and the temperature dependence of probe diffusivity is likely related to a sensitive balance in particular motility patterns of the particles closest to the probes.

Stokes-Einstein behavior

As described in the Introduction, single molecule experiments have suggested that if probe rotational diffusion constants change with temperature in a manner that tracks the viscosity change of the probe-free system with temperature, it can be assumed that the probe diffusion is mirroring the dynamics of the probe-free host. Our results bring into question this assumption, at least for translation, since we find evidence for enhanced (anisotropic) host translational diffusion that results in unexpected enhanced caging and slower translational diffusion of the probe than would be expected at a given temperature in the probe-free host. To further investigate how the enhanced diffusion of the system and decreased diffusion of the probe may manifest in experimental measurements, we investigate the Stokes-Einstein (SE) behavior of probe-bearing supercooled KA systems. The SE relation can be expressed as $D\eta a/T = c$ with D the translational diffusion constant of tracer particles, η the shear viscosity of the system, T temperature, a the size of the tracer particle, and c a constant. While the SE relation was derived for large, massive tracer particles in a system of much smaller and lighter particles, it holds well for a variety of systems.[48,59,60] For probe-free KA and similar systems, it is known that at high temperatures, SE behavior for translations is obeyed while at temperatures associated with the supercooled regime, SE behavior does not hold and c increases with decreasing temperature.[53,59,61–66] This is related to the fact that dynamic heterogeneities emerge and dynamic cooperativity becomes important in this temperature regime. As a result, D, reflective of the more mobile particles in the system, does not decrease with temperature as quickly as η, which probes the less mobile particles in the system. Because η has been shown to scale as τ_α, the SE relationship can also be expressed as $D\tau_\alpha a/T = c$, where τ_α is the alpha-relaxation of the system. Because it can be challenging to accurately determine shear viscosity in simulated supercooled liquids, we chiefly investigated the incarnation of the SE relation that uses τ_α rather than η. However, we did investigate both formulations of the SE relation for the probe-bearing systems under study using the shear viscosity of the probe-bearing systems calculated from the Einstein relations from the stress autocorrelation function via $\eta = \lim_{t\to\infty}(V/2k_BT)(d/dt)\langle(\int_{t_0}^{t_0+t} P_{xz}(t')dt')^2\rangle_{t_0}$ and find the same trends for both expressions.[67] First, the SE behavior of the system as a whole is investigated by examining the quantity $D_{\mathrm{A(p)}}\tau_{\alpha,\,\mathrm{A(p)}}\sigma_{\mathrm{AA}}/T^*$. This expression probes the SE behavior of the large A particles in the systems with $\sigma_{\mathrm{p}} = 1$–5. Figure 7(a) reveals that all of the investigated systems exhibit SE breakdown at low temperature and that the deviation from SE behavior is nearly identical regardless of probe size. This is consistent with Fig. 2(c), which reveals that $D_{\mathrm{A(p)}}$ increases at approximately the same rate as $\tau_{\alpha,\mathrm{A(p)}}$ decreases with increasing probe size. Figure 7(a) demonstrates this is true not just at $T^* = 0.48$ (Fig. 2(c)) but at all temperatures investigated.

A more relevant quantity for experiments follows the diffusion of the probe itself and compares it to the viscosity or alpha-relaxation time of the system. Therefore, we investigate the quantity $D_{\mathrm{p}}\tau_{\alpha,\,\mathrm{A(p)}}\sigma_{\mathrm{p}}/T^*$ (Fig. 7(b)). Examining this quantity suggests that SE breakdown is suppressed in all systems with probes of $\sigma_{\mathrm{p}} \geq 2$. This same behavior emerges if τ_α is replaced by η (data not shown). This *apparent* suppression of SE breakdown is also seen in the infinite limit of this system ($\tau_{\alpha,\mathrm{A(p)}}$ replaced by $\tau_{\alpha,\mathrm{A(p=1)}}$ or $\eta_{(\mathrm{p})}$ replaced by $\eta_{(\mathrm{p=1})}$), indicating that even without finite size effects the apparent suppression of SE breakdown would be seen if monitoring probe diffusion but system alpha-relaxation or viscosity. The apparent suppression of SE breakdown is consistent with the other findings in this study: because both alpha-relaxation time and viscosity of the system decrease slightly with increasing probe size (or stay constant in the limit of an infinite system) while the diffusion of the probe particle decreases relative to expectation based on size, the value of the investigated quantity decreases relative to expectation at a given temperature, leading to the *apparent* suppression of SE breakdown even while the system does exhibit SE breakdown for all probes investigated.

CONCLUSION

Experiments in which probe behavior is used to elucidate the behavior of a surrounding host system are

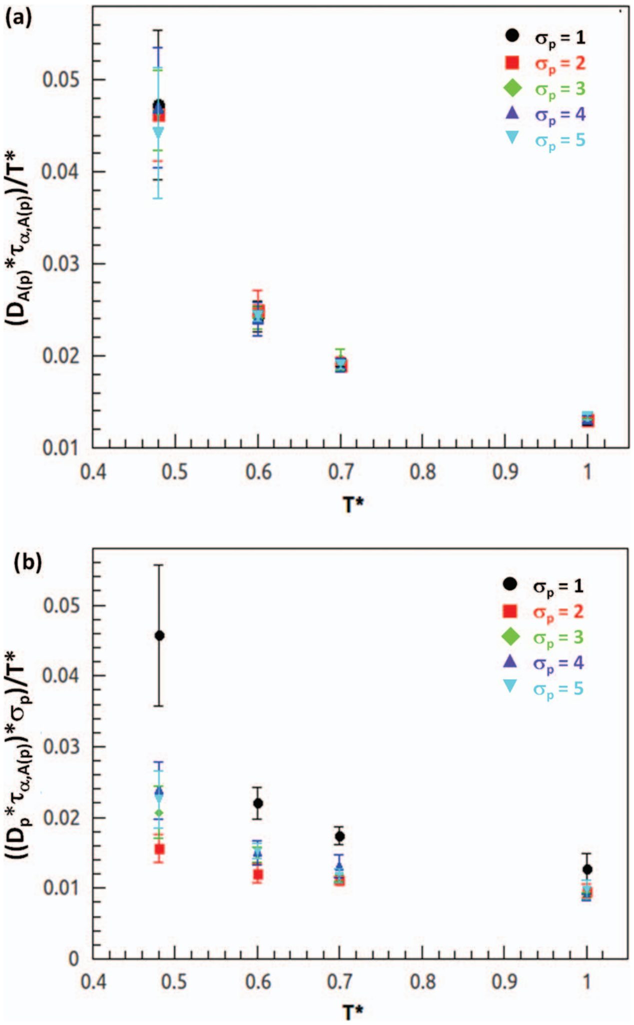

FIG. 7. (a) Stokes-Einstein behavior as revealed by examining A particles via $D_{A(p)}{}^*\tau_{\alpha,A(p)}/T^*$ in systems with probes of $\sigma_p = 1$ (black), $\sigma_p = 2$ (red), $\sigma_p = 3$ (green), $\sigma_p = 4$ (blue), $\sigma_p = 5$ (cyan). Stokes-Einstein breakdown is apparent in all systems and is not dependent on probe size. (b) Stokes-Einstein behavior as revealed by examining the diffusion of probe particles and alpha-relaxation of A particles via $(D_p{}^*\tau_{\alpha\ A(p)}{}^*\sigma_p)/T^*$ in systems with probes of $\sigma_p = 1$ (black), $\sigma_p = 2$ (red), $\sigma_p = 3$ (green), $\sigma_p = 4$ (blue), and $\sigma_p = 5$ (cyan). Stokes-Einstein breakdown appears suppressed when examining this quantity. In both (a) and (b), values are obtained by averaging D and τ_α values obtained from five independent simulations and error bars are standard deviations.

increasingly common. In the complex environments of supercooled liquids, where dynamic heterogeneities exist, probe behavior should not necessarily be expected to mirror host behavior. The assumption that probe behavior will mirror host behavior is a poor one for many reasons including that the probe may average over or alter dynamic heterogeneities in the system. Here, we investigate how probe behavior is altered in systems in which dynamics and dynamic heterogeneities are altered by the presence of the probe. In accordance with a previous study, we find that the presence of smooth probes larger than the host particles increases translational diffusion of the particles in the solvation shells near the probe.[41] Unexpectedly, we find that the probe does not exhibit enhanced translational diffusion as a result of the increased translational diffusion of the surrounding particles and instead exhibits suppressed translational diffusion. This occurs because the enhanced translational diffusion induced by the probe is anisotropic, with enhanced motility along the probe, promoting enhanced caging of the probe. Furthermore, we speculate that as a result of the competing effects from enhanced caging and enhanced host diffusion, while host behavior changes monotonically with probe size, probe behavior does not. In accordance with this finding, the temperature dependence of probe translational diffusion is found to deviate most from that of a probe-fee system for the modestly sized $\sigma_p = 2$ probe. As a result of the competing effects that allow for slowed probe diffusion in the background of enhanced system mobility, Stokes-Einstein breakdown as it would most likely be measured in a probe-bearing experiment appears strongly suppressed even while the host particles in the probe-bearing system experience the same deviations from SE behavior that would be seen in the absence of probes. This work points out the unintuitive ways in which probes may not only alter their surroundings but also then respond to those altered surroundings.

ACKNOWLEDGMENTS

The work was supported by National Science Foundation (NSF) CHE 0744322.

[1] M. D. Ediger, Annu. Rev. Phys. Chem. **51**, 99 (2000).
[2] R. Richert, J. Phys.: Condens. Matter **14**, R703 (2002).
[3] M. T. Cicerone and M. D. Ediger, J. Chem. Phys. **103**, 5684 (1995).
[4] M. T. Cicerone and M. D. Ediger, J. Chem. Phys. **104**, 7210 (1996).
[5] F. R. Blackburn, C. Y. Wang, and M. D. Ediger, J. Phys. Chem. **100**, 18249 (1996).
[6] R. Bohmer, G. Hinze, G. Diezemann, B. Geil, and H. Sillescu, Europhys. Lett. **36**, 55 (1996).
[7] R. Bohmer, R. V. Chamberlin, G. Diezemann, B. Geil, A. Heuer, G. Hinze, S. C. Kuebler, R. Richert, B. Schiener, H. Sillescu, H. W. Spiess, U. Tracht, and M. Wilhelm, J. Non-Cryst. Solids **235**, 1 (1998).
[8] U. Tracht, M. Wilhelm, A. Heuer, H. Feng, K. Schmidt-Rohr, and H. W. Spiess, Phys. Rev. Lett. **81**, 2727 (1998).
[9] U. Tracht, A. Heuer, and H. W. Spiess, J. Non-Cryst. Solids **235**, 27 (1998).
[10] E. Hempel, G. Hempel, A. Hensel, C. Schick, and E. Donth, J. Phys. Chem. B **104**, 2460 (2000).
[11] S. A. Reinsberg, X. H. Qiu, M. Wilhelm, H. W. Spiess, and M. D. Ediger, J. Chem. Phys. **114**, 7299 (2001).
[12] H. Sillescu, R. Bohmer, G. Diezemann, and G. Hinze, J. Non-Cryst. Solids **307-310**, 16 (2002).
[13] X. H. Qiu and M. D. Ediger, J. Phys. Chem. B **107**, 459 (2003).
[14] L. Wang and R. Richert, J. Chem. Phys. **120**, 11082 (2004).
[15] W. Huang and R. Richert, Philos. Mag. **87**, 371 (2007).
[16] J. R. Rajian and E. L. Quitevis, J. Chem. Phys. **126**, 224506 (2007).
[17] L. A. Deschenes and D. A. V. Bout, J. Phys. Chem. B **106**, 11438 (2002).
[18] R. Zondervan, F. Kulzer, G. C. G. Berkhout, and M. Orrit, Proc. Natl. Acad. Sci. U.S.A. **104**, 12628 (2007).
[19] S. A. Mackowiak, T. K. Herman, and L. J. Kaufman, J. Chem. Phys. **131**, 244513 (2009).
[20] S. A. Mackowiak, L. M. Leone, and L. J. Kaufman, Phys. Chem. Chem. Phys. **13**, 1786 (2011).
[21] G. Williams and P. J. Hains, Chem. Phys. Lett. **10**, 585 (1971).
[22] M. F. Shears and G. Williams, J. Chem. Soc., Faraday Trans. 2 **69**, 1050 (1973).
[23] F. R. Blackburn, M. T. Cicerone, G. Hietpas, P. A. Wagner, and M. D. Ediger, J. Non-Cryst. Solids **172**, 256 (1994).
[24] M. T. Cicerone, F. R. Blackburn, and M. D. Ediger, J. Chem. Phys. **102**, 471 (1995).
[25] G. Heuberger and H. Sillescu, J. Phys. Chem. **100**, 15255 (1996).
[26] W. Huang and R. Richert, J. Chem. Phys. **133**, 214501 (2010).
[27] S. Bhattacharyya and B. Bagchi, J. Chem. Phys. **106**, 1757 (1997).

[28] S. Bhattacharyya and B. Bagchi, J. Chem. Phys. **107**, 5852 (1997).

[29] F. L. Somer and R. Hernandez, J. Phys. Chem. B **104**, 3456 (2000).

[30] G. H. Koenderink, H. Y. Zhang, M. P. Lettinga, G. Nagele, and A. P. Philipse, Phys. Rev. E **64**, 022401 (2001).

[31] F. Ould-Kaddour and D. Levesque, Phys. Rev. E **63**, 011205 (2001).

[32] R. K. Murarka, S. Bhattacharyya, and B. Bagchi, J. Chem. Phys. **117**, 10730 (2002).

[33] G. H. Koenderink, H. Y. Zhang, D. Aarts, M. P. Lettinga, A. P. Philipse, and G. Nagele, Faraday Discuss. **123**, 335 (2003).

[34] A. J. Moreno and W. Kob, J. Chem. Phys. **121**, 380 (2004).

[35] A. J. Moreno and W. Kob, Europhys. Lett. **67**, 820 (2004).

[36] A. V. Popov, J. Melvin, and R. Hernandez, J. Phys. Chem. A **110**, 1635 (2006).

[37] R. A. L. Vallee, W. Paul, and K. Binder, J. Chem. Phys. **127**, 154903 (2007).

[38] F. Hofling, E. Frey, and T. Franosch, Phys. Rev. Lett. **101**, 120605 (2008).

[39] R. A. L. Vallee, W. Paul, and K. Binder, J. Chem. Phys. **132**, 034901 (2010).

[40] A. K. Tucker and R. Hernandez, J. Phys. Chem. A **114**, 9628 (2010).

[41] R. Zangi, S. A. Mackowiak, and L. J. Kaufman, J. Chem. Phys. **126**, 104501 (2007).

[42] W. Kob and H. C. Andersen, Phys. Rev. E **51**, 4626 (1995).

[43] W. Kob and H. C. Andersen, Phys. Rev. E **52**, 4134 (1995).

[44] W. Kob, C. Donati, S. J. Plimpton, P. H. Poole, and S. C. Glotzer, Phys. Rev. Lett. **79**, 2827 (1997).

[45] A. Mukherjee, S. Bhattacharyya, and B. Bagchi, J. Chem. Phys. **116**, 4577 (2002).

[46] B. Hess, C. Kutzner, D. van der Spoel, and E. Lindahl, J. Chem. Theory Comput. **4**, 435 (2008).

[47] E. Lindahl, B. Hess, and D. van der Spoel, J. Mol. Model. **7**, 306 (2001).

[48] J.-P. Hansen and I. R. McDonald, *Theory of Simple Liquids* (Academic, Burlington, 2006).

[49] W. Gotze, *Complex Dynamics of Glass-Forming Liquids: A Mode-Coupling Theory* (Oxford University Press, New York, 2009).

[50] W. Kob and H. C. Andersen, Phys. Rev. Lett. **73**, 1376 (1994).

[51] E. Flenner and G. Szamel, Phys. Rev. E **72**, 011205 (2005).

[52] E. Flenner and G. Szamel, Phys. Rev. E **72**, 031508 (2005).

[53] P. Bordat, F. Affouard, M. Descamps, and F. Muller-Plathe, J. Phys.: Condens. Matter **15**, 5397 (2003).

[54] D. Coslovich and G. Pastore, J. Chem. Phys. **127**, 124505 (2007).

[55] P. Scheidler, W. Kob, and K. Binder, Europhys. Lett. **59**, 701 (2002).

[56] P. Scheidler, W. Kob, and K. Binder, Eur. Phys. J. E **12**, 5 (2003).

[57] P. Scheidler, W. Kob, and K. Binder, J. Phys. Chem. B **108**, 6673 (2004).

[58] K. Watanabe, T. Kawasaki, and H. Tanaka, Nature Mat. **10**, 512 (2011).

[59] C. De Michele and D. Leporini, Phys. Rev. E **63**, 10 (2001).

[60] M. M. Kopswerkhoven and H. M. Fijnaut, J. Chem. Phys. **77**, 2242 (1982).

[61] R. Zangi and L. J. Kaufman, Phys. Rev. E **75**, 051501 (2007).

[62] S. K. Kumar, G. Szamel, and J. F. Douglas, J. Chem. Phys. **124**, 6 (2006).

[63] R. Yamamoto and A. Onuki, Phys. Rev. E **58**, 3515 (1998).

[64] R. Yamamoto and A. Onuki, Phys. Rev. Lett. **81**, 4915 (1998).

[65] J. Kim and T. Keyes, J. Phys. Chem. B **109**, 21445 (2005).

[66] K. Kim and S. Saito, J. Phys. Soc. Jpn. **79**, 093601 (2010).

[67] B. Hess, J. Chem. Phys. **116**, 209 (2002).